Supplementary Information:

Multi-component surface engineering of $Na_3V_2(PO_4)_2O_2F$ for low-temperature (-40 °C) sodium-ion batteries

Kunxiong Zheng,[†a] Shitan Xu,[†a] Yu Yao,[b] Dong Chen,[a] Lin Liu,[a] Chen Xu,[c] Yuezhan Feng,[d] Xianhong Rui*[a] and Yan Yu*[b]

[a.] School of Materials and Energy, Guangdong University of Technology, Guangzhou 510006, China. E-mail: xhrui@gdut.edu.cn

[b.] Hefei National Research Center for Physical Sciences at the Microscale, Department of Materials Science and Engineering, CAS Key Laboratory of Materials for Energy Conversion, University of Science and Technology of China, Hefei, Anhui 230026, China. E-mail: yanyumse@ustc.edu.cn

[c.] Academy for Advanced Interdisciplinary Studies, Southern University of Science and Technology, Shenzhen 518055, China

[d.] Key Laboratory of Materials Processing and Mold (Ministry of Education), Zhengzhou University, Zhengzhou 450002, China.

† These authors contributed equally to the work.

Experimental details

Synthesis of NVPOF@GO and MC-NVPOF

Graphene oxide (GO) prepared by modified Hummer method was treated under ultrasound for 2 h and stirred at room temperature for 1 h. Then, stoichiometric V_2O_5 and $C_6H_8O_7$ were added into the graphene oxide solution and stirred at 70 ℃ for 1.5 h . Immediately afterwards, 4.5 mmol $NH_4H_2PO_4$ and 1.5 mmol NaF were added into the solution and stirred for another 0.5 h. Thereafter the dark black solution was transfer to a microwave hydrothermal kettle and reacted at 170 ℃ for 4 h to achieve $Na_3V_2O_2(PO_4)_2F$@GO (denoted as NVPOF@GO). Subsequently, the NVPOF@GO was heated at 600 ℃ for 1.5 h under Ar/H_2 atmosphere to obtain the MC-NVPOF.

Material Characterization

X-ray diffraction (XRD) was tested using a Rigaku SmartLab polycrystal X-ray diffractometer with a Cu Kα radiation (λ=0.15418 nm) over a scan range of 10~70 ° (scan rate: 5° min^{-1}). The obtained XRD data were analyzed with the software Jade 6.0. Thermogravimetric analysis (TGA) was carried out using STA 449C in air atmosphere over the range of 25~600 °C (heating rate: 10 °C min^{-1}). Fourier transform infrared (FTIR) spectra, Raman spectra X-ray photoelectron spectroscopy (XPS) were operated on Nicolet iS50R, LabRAM HR800 and Escalab 250 Xi, respectively. The morphology and microstructure were characterized by a Hitachi SU-8220 field-emission scanning electron microscope and a JEM-2100F transmission electron microscope.

Electrochemical measurements

The CR2032 coin cells were fabricated with the cathode materials mentioned above as the working electrode, metallic sodium as both the counter and reference electrode, glass fiber as the separator, and 1 mol L^{-1} $NaClO_4$ in mixed solvents of propylene carbonate (PC)/ethylene carbonate (EC) (1:1 in volume) with an addition of 5% FEC as the electrolyte used at room temperature; 1 mol L^{-1} $NaClO_4$ in DME as electrolyte used at low temperature. The cathode was fabricated on Al foil by coating mixed slurry of 70 wt% active material, 20 wt% Super P, and 10 wt% binder (polyvinylidene fluoride) in N-methyl- pyrrolidone (NMP) solvent. The slurry was stirred for 48 h and then coated onto the aluminum foil (Ø =12 mm). After that, the electrode was dried for overnight (12 h) under vacuum at 60 ℃. The mass loading of active materials is 0.7~0.8 mg cm^{-2}. The electrochemical behaviors of the as-prepared electrodes for SIBs were measured in CR2032 type coin-cells, which were assembled in an argon filled glove box (H_2O and O_2 content less than 0.1 ppm). The cells were test on a battery testing system (Neware, Shenzhen, China) between 3~4.3 V versus Na/Na^+ at room temperature and 2.5~4.3 V for subzero temperature (-40 ^oC). The cyclic Voltammetry (CV) and electrochemical impedance spectra (EIS) were measured on an electrochemistry workstation (CHI-660e).

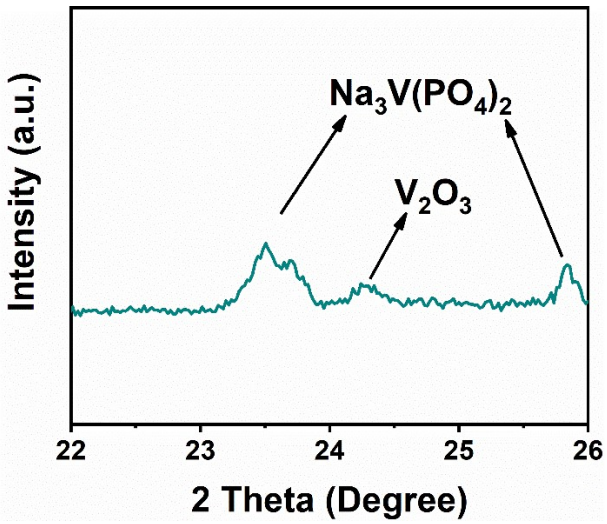

Fig. S1 Local enlargement of XRD pattern of the MC-NVPOF

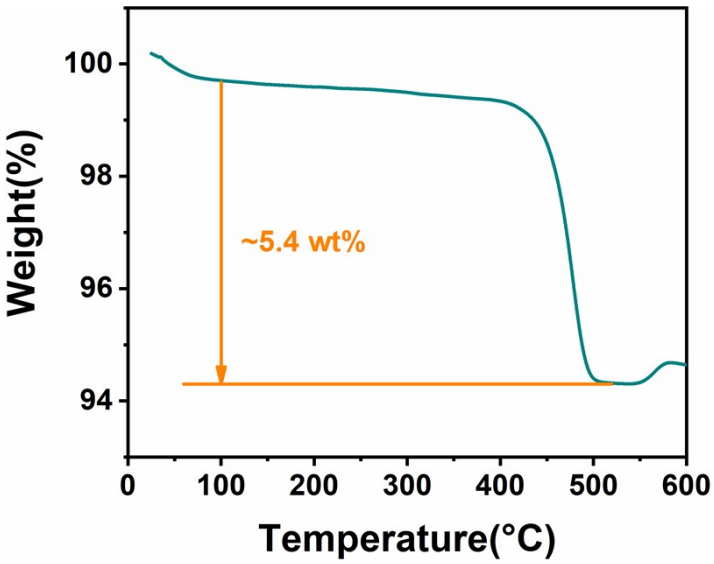

Fig. S2 TGA curve of the MC-NVPOF material

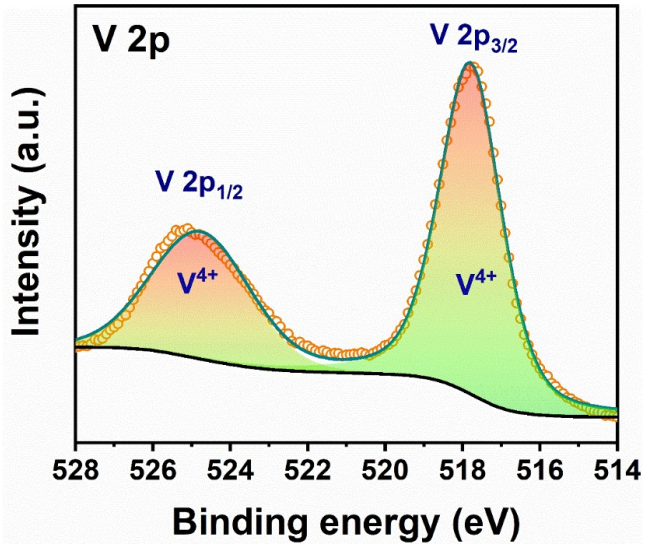

Fig. S3 High-resolution V 2p spectrum of NVPOF@GO.

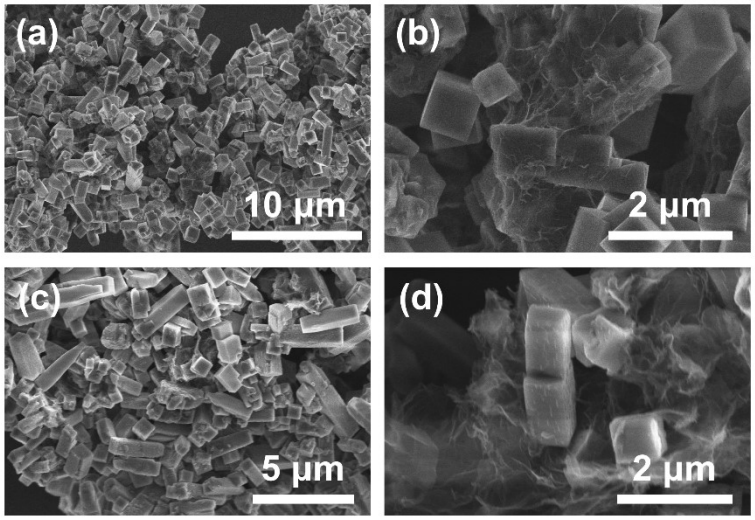

Fig. S4 SEM morphology of (a and b) NVPOF@GO and (c and d) MC-NVPOF at different magnifications.

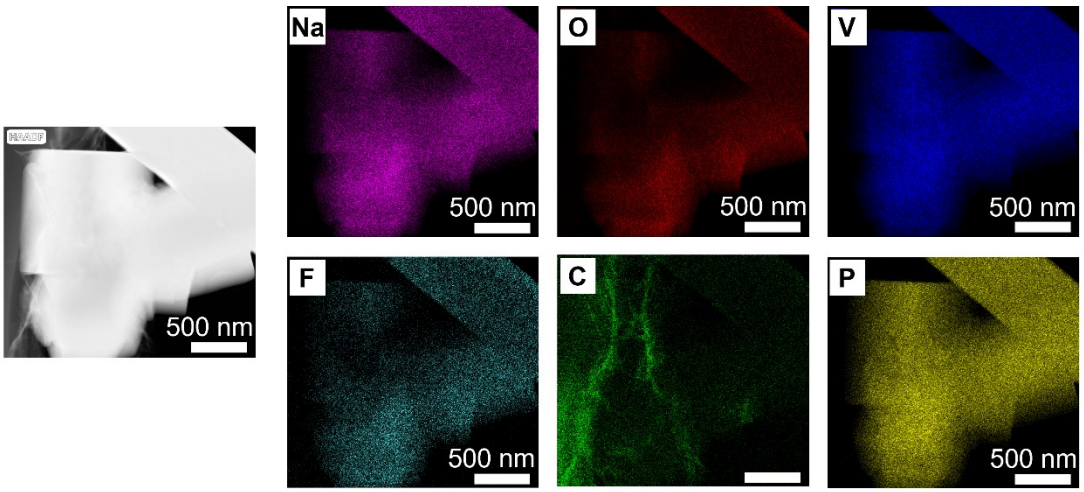

Fig. S5 EDS mapping images of the MC-NVPOF.

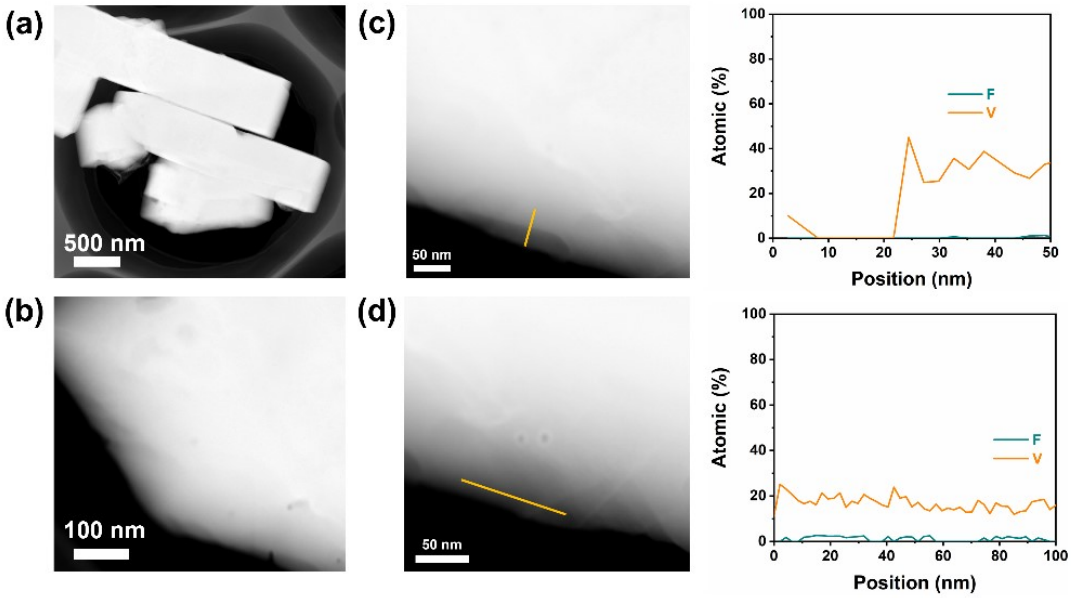

Fig. S6 (a, b) TEM images of the MC-NVPOF and the corresponding line scan and atomic distribution of F at the surface edge along (c) the width direction and (d) the length direction.

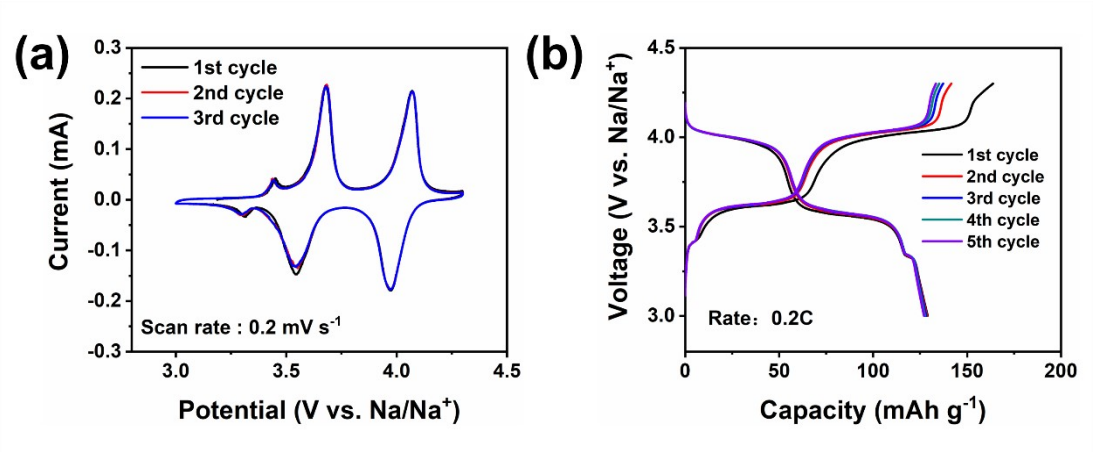

Fig. S7 (a) CV curve at the scan rate of 0.2 mV s^{-1} and (b) the first five cycles of GCD curve at 0.2 C.

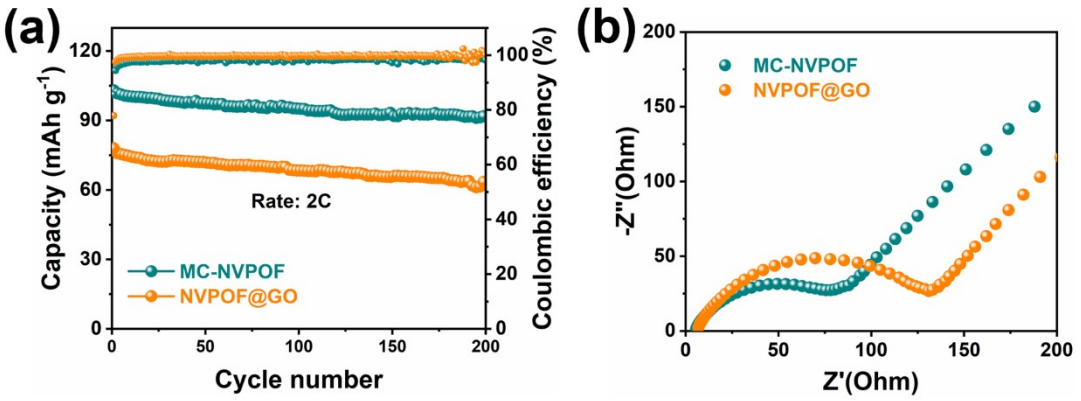

Fig. S8 (a) Cycling performance of MC-NVPOF and NVPOF@GO at 2 C, (b) EIS of MC-NVPOF and NVPOF@GO.

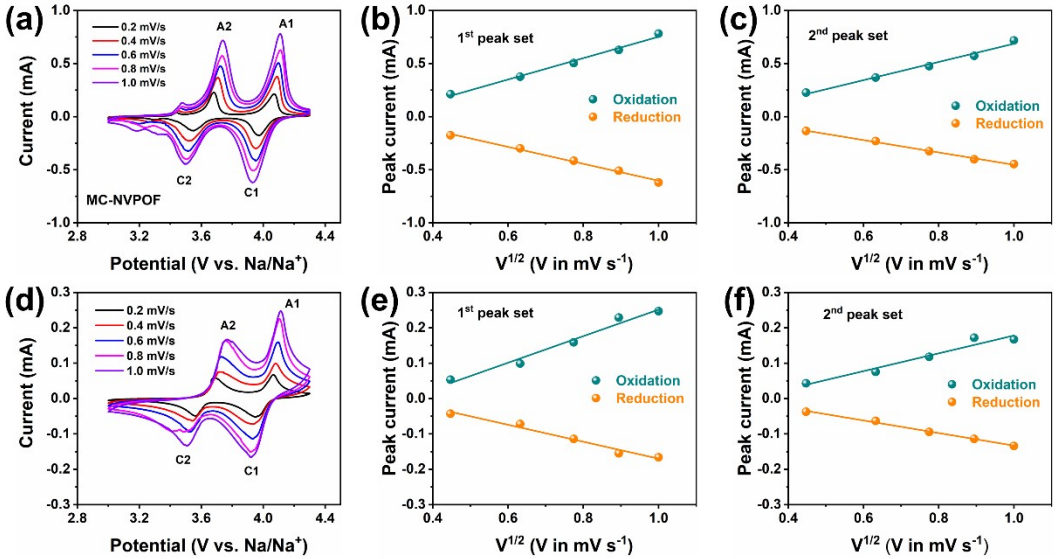

Fig. S9 (a) CV curves for the MC-NVPOF nanocomposite at different scan rates. The plots between the square root of the scan rate and the peak current for (b) A1, C1 peaks and (c) A2, C2 peaks. (d) CV curves for the NVPOF@GO nanocomposite at different scan rates. The plots between the square root of the scan rate and the peak current for (e) A1, C1 peaks and (f) A2, C2 peaks.

As the scan rate (v) increases, the height and area of the CV peaks continuously enlarge. The above peaks show the linear relationship between the peak current (i_p) and the square root of the scan rate ($v^{1/2}$), which implies that the electrochemical process of NVPOF-based cathodes is diffusion dominant as the intercalated compound. Then, the apparent Na^+ diffusion coefficient ($D_{app,Na}$) can be calculated by Randles-Sevcik equation as follow:

$$i_p = (2.65 \times 10^5) n^{3/2} S D_{Na^+}^{1/2} C_{Na^+} v^{1/2}$$

where n represents the number of electrons transferred in the redox event, and the S indicates the surface area of the NVPOF electrode, C_0 represented of concentration of Na^+ in the NVPOF, respectively.

The $D_{app,Na}$ of NVPOF@GO is determined to be 3.33×10^{-12}, 1.35×10^{-12}, 1.49×10^{-12}, and 7.39×10^{-13} cm^2 s^{-1} for A1, C1, A2, and C2 peaks, respectively. Significantly, $D_{app,Na}$ of MC-NVPOF is greatly increasing to 2.29×10^{-11}, 1.50×10^{-11}, 1.74×10^{-11}, and 8.00×10^{-12} cm^2 s^{-1} for A1, C1, A2, and C2 peaks, respectively.

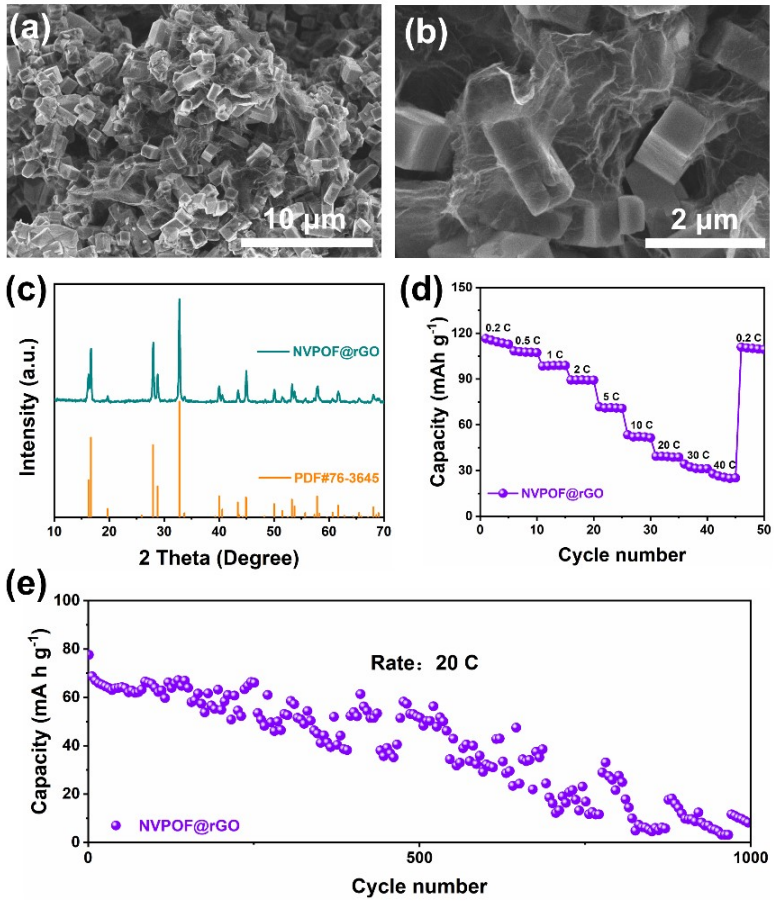

Fig. S10 (a, b) SEM images, (c) XRD pattern, (d) rate performance and (e) cycling performance of the NVPOF@rGO cathode at 20 C.

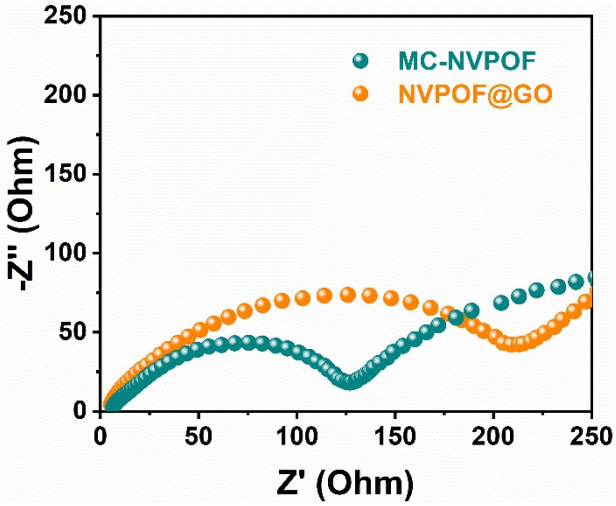

Fig. S11 EIS of MC-NVPOF and NVPOF@GO after cycling.

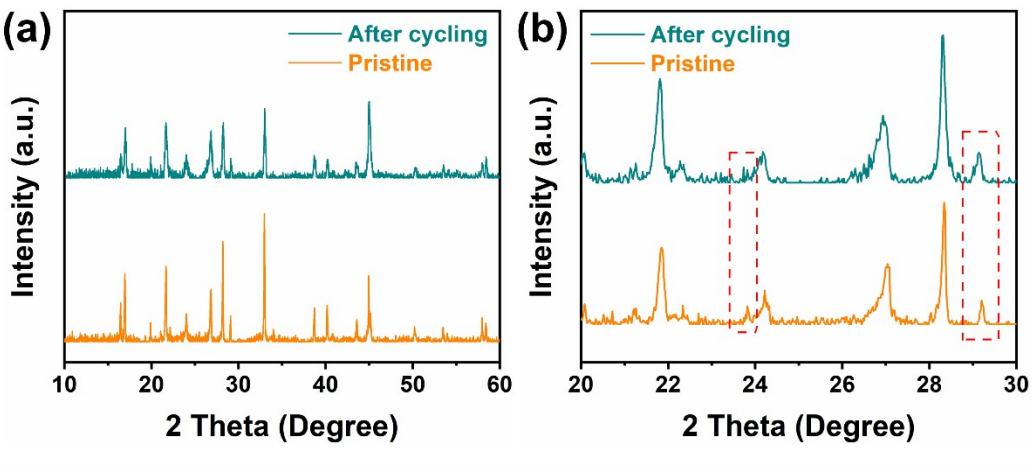

Fig. S12 Ex-situ XRD patterns of (a) MC-NVPOF and (b) NVPOF@GO electrode (pristine and after cycling).

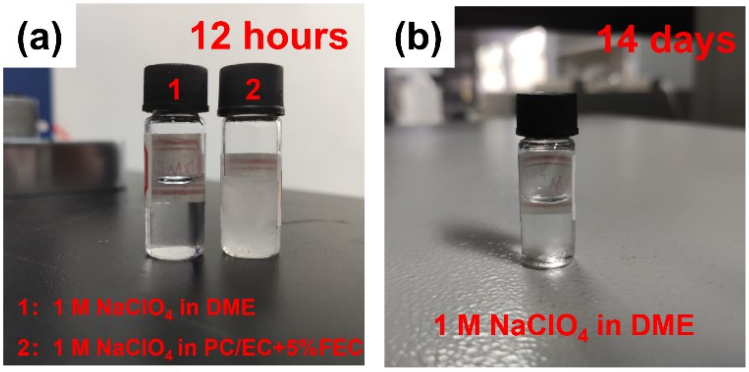

Fig. S13 Digital photos of 1M $NaClO_4$ in DME and 1M $NaClO_4$ in PC:EC + 5% FEC electrolytes placed at -40 ℃ for (a) 12 h and (b) 14 days.

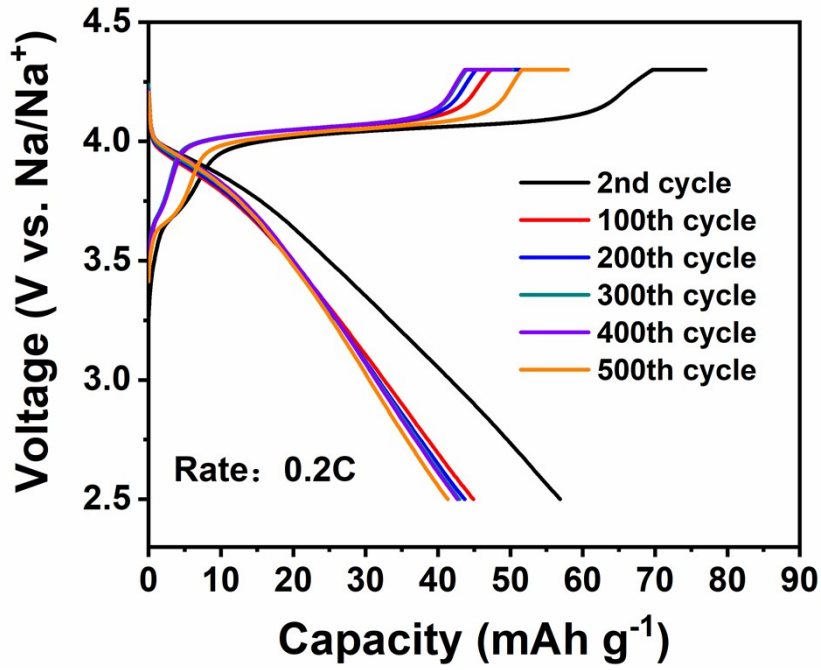

Fig. S14 The charge-discharge curves of MC-NVPOF at 3 C and -40 °C.

Table S1. A comparison of the LT performance of our MC-NVPOF with other cathodes for SIBs.

Cathode	Capacity	Lifetime	Temperature	Ref.
MC-NVPOF	88 mA h g^{-1}@0.2 C	500 (3 C)	-40 °C	**This work**
$Na_3V_2(PO_4)_2O_2F$	59 mA h g^{-1}@0.5 C	200 (0.2 C)	-25 °C	[1]
$Na_3V_2(PO_4)_2F_3$	50 mA h g^{-1}@0.1 C	/	-20 °C	[2]
$Na_3V_2(PO_4)_3$	50 mA h g^{-1}@0.2 C	80 (0.2 C)	-40 °C	[3]
$Na_3V_{1.98}Mn_{0.02}(PO_4)_2F_3$	80 mA h g^{-1}@0.2 C	400 (0.5 C)	-25 °C	[4]
$Na_{0.66}[Mn_{0.66}Ti_{0.34}]O_{2-x}F_x$ (x<0.1)	60 mA h g^{-1}@0.2 C	140 (0.2 C)	-20 °C	[5]

1. X. X. Zhao, Z. Y. Gu, W. H. Li, X. Yang, J. Z. Guo and X. L. Wu, *Chemistry*, 2020, **26**, 7823-7830.
2. J. Hwang, K. Matsumoto and R. Hagiwara, *Adv. Energy Mater.*, 2020, **10**, 2001880.
3. A. C. Thenuwara, P. P. Shetty, N. Kondekar, C. Wang, W. Li and M. T. McDowell, *J. Mater. Chem. A*, 2021, **9**, 10992-11000.
4. Z. Y. Gu, J. Z. Guo, Z. H. Sun, X. X. Zhao, X. T. Wang, H. J. Liang, B. Zhao, W. H. Li, X. M. Pan and X. L. Wu, *Small*, 2021, **17**, e2102010.
5. Q.-C. Wang, Q.-Q. Qiu, N. Xiao, Z.-W. Fu, X.-J. Wu, X.-Q. Yang and Y.-N. Zhou, *Energy Storage Mater.*, 2018, **15**, 1-7.